Preprint-00

Lyman-Alpha Forest Power Spectrum

Avery Meiksin[1], Martin White[2]
[1] *Institute for Astronomy, University of Edinburgh, Blackford Hill, Edinburgh EH9 3HJ, UK*
[2] *Departments of Astronomy and Physics, University of California, Berkeley, CA 94720, USA*

9 January 2003

ABSTRACT
We look at the effects on the flux power spectrum of fluctuations in the UV background due to a finite number of sources.

Key words: methods: numerical – intergalactic medium – quasars: absorption lines

1 INTRODUCTION

Due in large part to insights gained from hydrodynamical simulations of structure formation in the universe (Cen et al. 1994; Zhang, Anninos & Norman 1995; Hernquist et al. 1996; Zhang et al. 1997; Bond & Wadsley 1997; Theuns, Leonard & Efstathiou 1998a) the Lyα forest, as measured in high redshift Quasi-Stellar Object (QSO) spectra, has emerged as one of our premier probes of the universe at high redshift. It is now believed that photoionization equilibrium for the gas results in a tight density–temperature relation for the absorbing material with the neutral hydrogen density proportional to the baryon density squared (REFS). Since pressure filtering is subdominant to thermal broadening (REF), the neutral hydrogen density closely traces the total matter density (squared) on the scales relevant to the forest ($0.1 - 10\,h^{-1}$Mpc). The structure in QSO absorption thus traces, in a calculable way, slight fluctuations in the matter density of the universe back along the line of sight to the QSO, with most of the Lyα forest arising from overdensities of a few times the mean density.

While much work has been done on the physics of the Lyα forest and the cosmology which can be extracted, the role of fluctuations in the UV background on the absorption properties of the Lyα forest have been largely unexplored (see Zuo 1992; Fardal & Shull 1993; Croft et al. 1999, 2002; Gnedin & Hamilton 2002). In this paper, we investigate the effect of the fluctuations on the 2-pt flux distribution (the power spectrum) of the Lyα forest. This extends our earlier work on the 1-pt distribution function reported in Meiksin & White (2002; hereafter Paper I).

2 NUMERICAL SIMULATIONS

To investigate the effects of UV background fluctuations on the power spectrum of the Lyα forest, we have performed simulations of 3 different cosmological models within the ΛCDM family. In each case we used pure dark matter simulations, mimicking the temperature of the gas using a polytropic equation of state and assuming gas and dark matter have the same spatial distribution. This has been shown (Gnedin & Hui 1998; Petitjean, Mücket & Kates 1995; Croft et al. 1998; Meiksin & White 2001) to produce results comparable to the full hydrodynamical simulations at the level of 10 per cent. The agreement is expected to be even better on the large scales of interest to this work. The parameters for the simulations can be found in Table 1 and a description of the parallel PM code used can be found in Paper I. In each case we used 512^3 particles and a 1024^3 force mesh, in a cubic box with (comoving) side length $25\,h^{-1}$Mpc. Convergence tests, described in the Appendix, suggest that this is adequate for our purposes.

Model	Ω_M	Ω_Λ	$\Omega_b h^2$	h	n	σ_8
1	0.30	0.70	0.02	0.70	1.05	0.970
2	0.35	0.65	0.02	0.70	0.95	0.885
3	0.40	0.60	0.02	0.55	1.10	0.902

Table 1. Parameters for the cosmological models. Ω_M is the total mass density parameter, Ω_Λ the cosmological constant density parameter, Ω_b the baryonic mass fraction, $h = H_0/100\,\mathrm{km\,s^{-1}\,Mpc^{-1}}$, where H_0 is the Hubble constant at $z = 0$, n the slope of the primordial density perturbation power spectrum, σ_8 the fluctuation normalization at $z = 0$ in a sphere of radius $8h^{-1}$ Mpc.

Given a set of final particle positions and velocities, we compute the spectra as follows. First the density and density-weighted line-of-sight velocity are computed on a grid (using CIC interpolation) and Gaussian smoothed using FFT techniques in order to adequately sample the velocity field. This forms the fundamental data set. A regular grid of 32×32 sightlines is drawn through the box, parallel to the box sides.

z	$\tau_{\rm eff}$	r_0	N_0	$N_{\rm box}$
8.5	6.76	?	?	?
6.0	2.34	11.6	0.5	1.2
5.5	1.82	23.9	5.1	1.4
5.0	1.38	49.1	49	1.5
4.0	0.73	179	3190	2.1

Table 2. Some of the output times for the simulations. For each redshift the mean opacity, $\tau_{\rm eff}$, the attenuation length, r_0 in comoving h^{-1} Mpc, and the mean number of sources per attenuation volume, N_0, is listed for Model 1. The last column, $N_{\rm box}$, shows the number of sources in the simulation volume of side $25\,h^{-1}$Mpc (comoving).

Along each sightline we integrate (in real space) to find $\tau(u)$ at a given velocity u. Specifically we define

$$\tau(u) = \int dx\, A(x) \left[\frac{\rho(x)}{\bar\rho}\right]^2 T(x)^{-0.7} b^{-1} e^{-(u-u_0)^2/b^2} \qquad (1)$$

where $u_0 = xaHL_{\rm box} + v_{\rm los}$ and $b = \sqrt{2k_BT/m_{\rm H}}$ is the Doppler parameter, where $m_{\rm H}$ is the mass of a hydrogen atom. The flux at velocity u is $\exp[-\tau]$. The integration variable x indicates the distance along the box in terms of the expansion velocity across the box. In evaluating Eq. (1) we assume a power-law relation between the gas density and temperature

$$T \equiv T_0 \left(\frac{\rho}{\bar\rho}\right)^{\gamma-1} \qquad (2)$$

In practice, T_0 and γ will depend on the reionization history of the IGM, but we shall fix $T_0 = 2\times10^4$K and $\gamma = 1.5$ throughout as described in Paper I.

In terms of the baryon density parameter Ω_b, hydrogen baryonic mass fraction X, the metagalactic photoionization rate Γ_{-12}, in units of $10^{-12}\,{\rm s}^{-1}$, and the number f_e of electrons per hydrogen nucleus, the function $A(x)$ is given by:

$$A = 18.0 f_e \left(\frac{X}{0.76}\right)\left(\frac{\Omega_b h^2}{0.02}\right)\Gamma_{-12}^{-1} L_{\rm box}(1+z)^5, \qquad (3)$$

where Γ_{-12} is evaluated at position x, $L_{\rm box}$ is in Mpc and b in eq. (1) is in $\rm km\,s^{-1}$. For both constant and spatially varying $A(x)$ we scale the final τ so that the mean opacity follows (REF)

$$\tau_{\rm eff} \equiv -\ln\left\langle e^{-\tau}\right\rangle = 0.0028\ (1+z)^{3.46} \qquad . \qquad (4)$$

Values for $\tau_{\rm eff}$ at each of the outputs of the simulation can be found in Table 2.

3 UV BACKGROUND FROM SOURCES

We need to assign luminosities to halos to compute $A(x)$. It is most natural to take the $N_{\rm box}$ most massive sources in the box, in decreasing order of mass, and assign them luminosities. This can be done in a number of ways.

First we could equate the cumulative mass distribution to the cumulative luminosity distribution to assign luminosities.

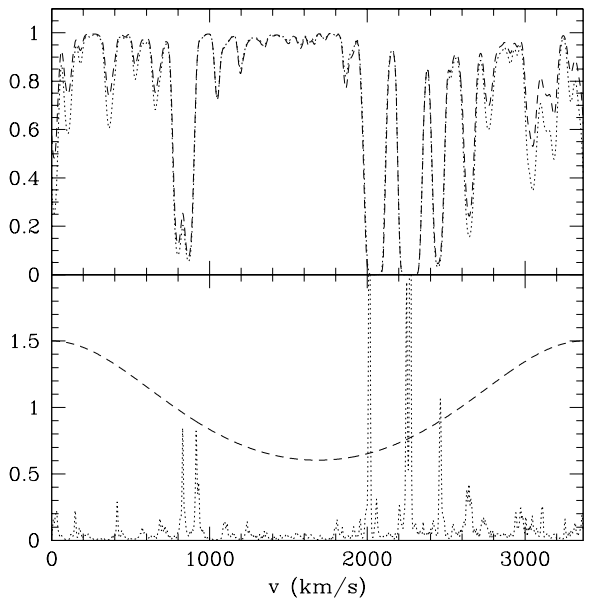

Figure 1. A simulated spectrum from a 'typical' sightline at z=5 from Model 1. The upper panel shows the spectrum with a uniform ionizing background ($A(x) \equiv$const, dashed) and where the UV background comes from a single source situated at the center of the box (dotted). The lower panel shows $0.1 \times \rho/\bar\rho$ (dotted) and $A(x)/\bar A$ (dashed) for the single source case.

Second, we could take the most massive halos in the simulation and measure their velocity dispersions then convert these to black hole masses using (Tremaine et al. 2002)

$$M_{BH} = 10^8\, M_\odot \left(\frac{\sigma}{200{\rm km\,s^{-1}}}\right)^4 \qquad (5)$$

The Eddington luminosity scales as the mass of the QSO, so we could take $L \propto \sigma^4$ also.

Finally, we could notice that $N_{\rm box}$ is a very small number. So we could just pick flux ratios between the first few most massive sources and set the overall scaling to get $\tau_{\rm eff}$ right.

4 HISTORY

Avery, you know the history and context here better than I do. We probably need to have some discussion somewhere in the paper about what has gone before and where we differ/do better. I've put the following in as a placeholder for now.

Zuo (1992) and Fardal & Shull (1993) did randomly distributed clouds and J fluctuations. Croft et al. (1999) looked at whether UVBG fluctuations and uniform IGM could give spectra like what is observed (no) and how big an effect putting fluctuating J into observed spectra was (their Fig. 12). Croft et al. (2002) took halos in the simulation, set $L \propto$SFR and added a uniform component to look at effect on spectra and $P(k)$ at $z \sim 3$ (their Figs. 11 and 12). Finally Gnedin & Hamilton (2002) discuss fluctuating UVBG using hydro simulations

with radiative transfer. They show UVBG fluctuations are a small effect on the power spectrum, but cause an underestimate of the photo-ionization rate by $\mathcal{O}(20\%)$.

ACKNOWLEDGMENTS

M. White was supported by the NSF and NASA. Parts of this work were done on the IBM-SP2 at the National Energy Research Scientific Computing Center.

APPENDIX A: CONVERGENCE TESTS

Even including only gravitational physics, simulations of the Lyα forest are restricted by two size constraints. High spatial resolution is required to resolve the structure of the absorbers, while a large box size is required both to capture the large-scale power which will affect the velocity widths of the absorption lines as well as to obtain a fair sample of the universe. Although a small box may be adequate to resolve the line structure, if the box is too small the fluctuations corresponding to the scale of the box will become nonlinear, in which case the results are no longer representative of the cosmological model simulated. These numerical effects have been investigated in different contexts by a number of authors (see references in McDonald 2001 for example).

To investigate these effects of numerical resolution further we chose a relatively large box, $30\,h^{-1}$Mpc (comoving) on a side, and simulated the concordance cosmology using 128^3, 256^3 or 512^3 particles (corresponding to 256^3, 512^3 and 1024^3 mesh cells). At the high redshifts of interest to us the fundamental mode of the box is safely in the linear regime, suggesting that the simulation represents a fair sample of the universe. To isolate the effects of numerical resolution from sample variance, we sampled the initial conditions starting at low-k and moving 'outwards' to higher k so that the initial phases and amplitudes of the common modes were identical from simulation to simulation.

The 3D matter power spectrum (not shown) exhibits the expected behaviour, with the higher resolution simulations having progressively more small-scale power. At $z = 5$ the fundamental mode is safely in the linear regime, with $\Delta^2(k_{\rm fund}) \simeq 0.04$, and the mesh scale is non-linear with $\Delta^2(k_{\rm mesh}) > 10$. The fitting formula of Peacock & Dodds (1996) underestimates the non-linear power by $\mathcal{O}(50)$ per cent. Fig. A1 shows the 1D matter power spectrum, in real space. This is an integral of the 3D spectrum over wavenumbers greater than the 1D wavenumber under consideration:

$$\frac{kP(k)}{\pi} = k\int_k^\infty \frac{dy}{y^2}\,\Delta^2_{3D}(y) \qquad . \tag{A1}$$

We find that the numerical results are relatively well fit by the Peacock & Dodds (1996) formalism, if we filter the 3D power spectrum, $\Delta^2_{3D}(k)$, with a Gaussian filter of FWHM 3.2 mesh cells (plotted as the solid line for the highest resolution run) to approximate the finite force resolution of the PM code.

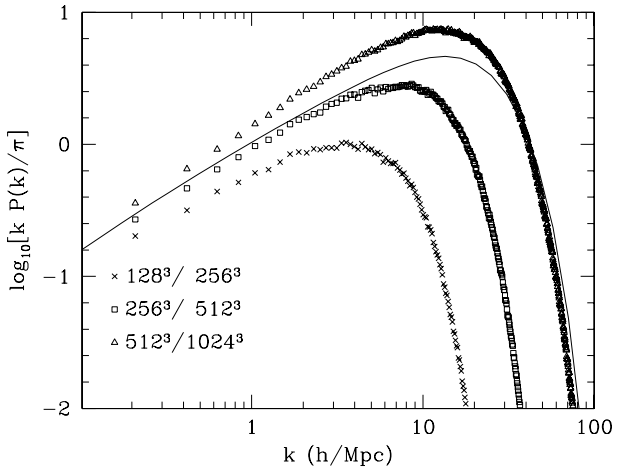

Figure A1. The (real space) 1D matter power spectrum in the concordance cosmology at $z = 5$ from our resolution sequence with 128^3, 256^3 and 512^3 particles and force meshes of 256^3, 512^3 and 1024^3. The solid line shows the predicted 1D spectrum, using the Peacock & Dodds (1996) fitting formulae for the 3D matter power spectrum, Eq. A1, and a Gaussian filtering of 3 mesh cells (FWHM).

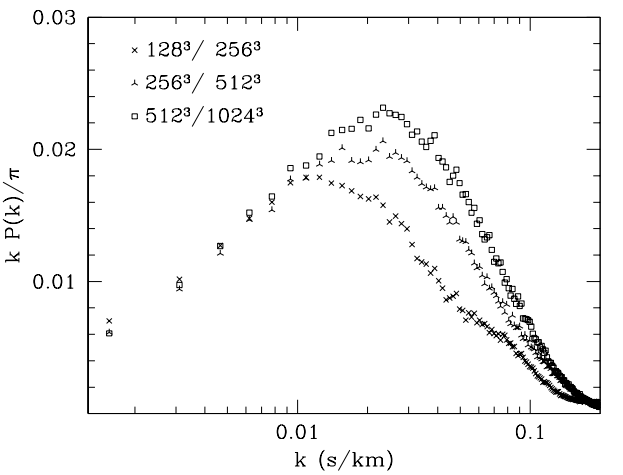

Figure A2. The 1D flux power spectrum in the concordance cosmology at $z = 5$ from our resolution sequence with 128^3, 256^3 and 512^3 particles and force meshes of 256^3, 512^3 and 1024^3. The box size in each run is $30\,h^{-1}$Mpc. These results indicate that our highest resolution runs are converged at better than the 10% level (in power).

Note that missing high-k power in the lower resolution simulations biases the 1D power spectrum low over the whole k-range plotted since much of the long-wavelength power comes from aliasing of 3D short wavelength power. Finally we show in Fig. A2 the power spectra of the flux produced by these 3 runs. From these results we infer that, for the relatively high redshifts of interest, a $30\,h^{-1}$Mpc box with 512^3 particles and

a 1024^3 force mesh produces spectra converged to better than the 10 per cent level. Similar conclusions were found by McDonald (2001), though our convergence is not quite at the level quoted therein. The convergence becomes fractionally better if we increase T_0 or decrease γ. It becomes only slightly worse if we lower T_0 to 10^4K. A further sequence reducing the box size (not shown here) suggests that we can safely reduce the volume simulated to a box of side $25\,h^{-1}$Mpc if we are interested in the Lyα forest at high redshift. This makes the mesh scale slightly smaller, capturing the features in the forest slightly better, thus we have used $25\,h^{-1}$Mpc thoughout.

REFERENCES

Bond J. R., Wadsley J. W., 1997, in Petitjean P., Charlot S., eds, Structure and Evolution of the Intergalactic Medium from QSO Absorption Line Systems. Editions Frontières, Paris, p. 143
Bryan G. L., Machacek M., Anninos P., Norman M. L., 1999, ApJ, 517, 13
Cen R., Miralda-Escudé J., Ostriker J. P., Rauch M., 1994, ApJ, 437, L9
Croft R.A.C., Weinberg D.H., Pettini M., Hernquist L., Katz N., 1999, ApJ, 520, 1
Croft R.A.C., Hernquist L., Springel V., Westover M., White M., 2002, ApJ, 580, 634
Croft R.A.C., Weinberg D. H., Katz N., Hernquist L., 1998, ApJ, 495, 44
Davé R., Hernquist L., Weinberg D. H., Katz N., 1997, ApJ, 477, 21
Fardal M., Shull M., 1993, ApJ, 415, 524
Gnedin N. Y., Hui L., 1998, MN, 296, 44
Gnedin N.,Y., Hamilton A.J.S., 2002, MNRAS, 334, 107
Hernquist L., Katz N., Weinberg D., Miralda-Escudé J., 1996, ApJ, 457, L51
Hui L., Gnedin N. Y., 1997, MN, 292, 27
Machacek M. E., Bryan G. L., Meiksin A., Anninos P., Thayer D., Norman M. L., Zhang Y., 2000, ApJ, 532, 118 (M00)
McDonald P., 2001, preprint [astro-ph/0108064]
Meiksin A., 1994, ApJ, 431, 109
Meiksin A., 2000, MN, 314, 566
Meiksin A., White M., Peacock J. A., 1999, MNRAS, 304, 851
Meiksin A., Bryan G. L., Machacek M. E., 2000, MNRAS, submitted
Peacock J.A, Dodds S.A., 1996, MNRAS, 280, 19
Petitjean P., Mücket J. P., Kates R. E., 1995, A&A, 295, L9
Ricotti M., Gnedin N., Shull J.M., 2000, 534, 41
Zhang Y., Anninos P., Norman M. L., 1995, ApJ, 453, L57
Zhang Y., Anninos P., Norman M. L., Meiksin A., 1997, ApJ, 485, 496
Zhang Y., Meiksin A., Anninos P., Norman M. L., 1998, ApJ, 495, 63